Title	Analysis of reactive astrocytes and NG2 proteoglycan in ex vivo rat models of spinal cord injury
Author(s)	Patar, Azim; Dockery, Peter; Howard, Linda; McMahon, Siobhan
Publication Date	2018-09-26
Publication Information	Patar, Azim, Dockery, Peter, Howard, Linda, & McMahon, Siobhan. (2019). Analysis of reactive astrocytes and NG2 proteoglycan in ex vivo rat models of spinal cord injury. Journal of Neuroscience Methods, 311, 418-425. doi: https://doi.org/10.1016/j.jneumeth.2018.09.027
Publisher	Elsevier
Link to publisher's version	https://doi.org/10.1016/j.jneumeth.2018.09.027
Item record	http://hdl.handle.net/10379/15295
DOI	http://dx.doi.org/10.1016/j.jneumeth.2018.09.027

Analysis of reactive astrocytes and NG2 proteoglycan in *ex vivo* rat models of spinal cord injury

AUTHOR(S): Azim Patar[a,d], Peter Dockery[b], Linda Howard[cβ], Siobhan McMahon[aβ*]

AFFILIATION(S): [a]Discipline of Anatomy and NCBES Galway Neuroscience Centre, College of Medicine Nursing and Health Sciences, National University of Ireland Galway, Ireland; [b]Discipline of Anatomy, College of Medicine Nursing and Health Sciences, National University of Ireland Galway, Ireland; [c]Regenerative Medicine Institute (REMEDI), College of Medicine Nursing and Health Sciences, National University of Ireland Galway, Ireland;[d]Department of Neuroscience, School of Medical Sciences, Universiti Sains Malaysia, Malaysia.

[β]Linda Howard and Siobhan S. McMahon should be considered joint senior authors

*CORRESPONDING AUTHOR: Dr Siobhan McMahon, Discipline of Anatomy and NCBES Galway Neuroscience Centre, College of Medicine Nursing and Health Sciences, National University of Ireland Galway, Ireland. EMAIL: siobhan.mcmahon@nuigalway.ie TEL: +353 91492838. FAX: Fax: +353 91 494520

GRAPHICAL ABSTRACT

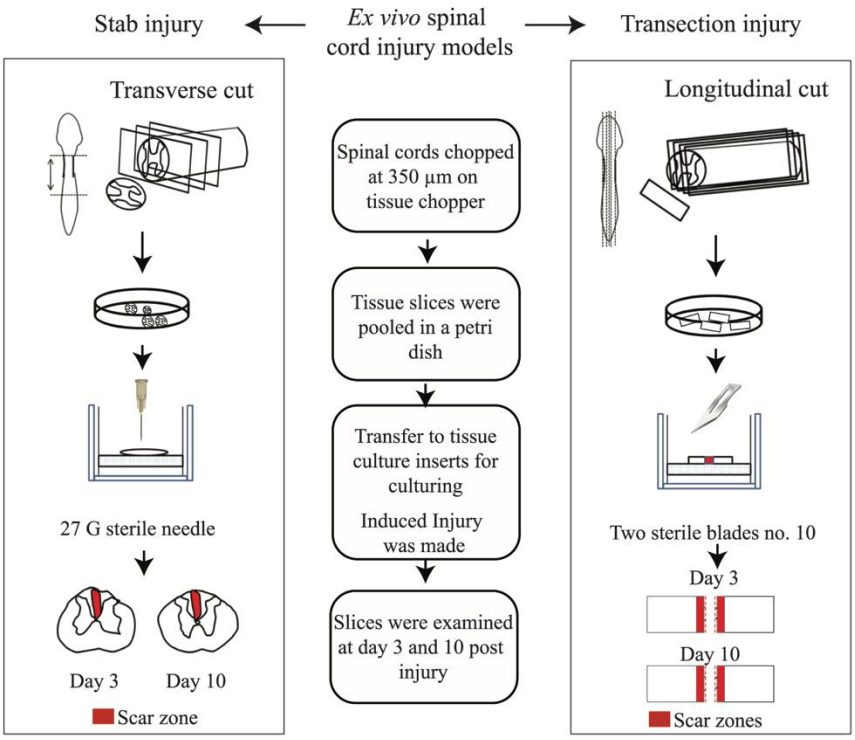

HIGHTLIGHTS

- The volume fraction of reactive astrocytes and NG2 proteoglycans increased significantly between day 3 and day 10 post injury in both *ex vivo* models.
- *Ex vivo* spinal cultures can be used as a platform for studying glial scarring and potential SCI treatments
- This culture system fulfilled the concept of replacement, reduction and refinement of animal use in SCI research models.

ABSTRACT

Background: The use of animals to model spinal cord injury (SCI) requires extensive post-operative care and can be expensive, which makes an alternative model extremely attractive. The use of *ex vivo* slice cultures is an alternative way to study the pathophysiological changes that can mimic *in vivo* conditions and support the 3Rs (replacement, reduction and refinement) of animal use in SCI research models. **New Method**: In this study the presence of reactive astrocytes and NG2 proteoglycans was investigated in two *ex vivo* models of SCI; stab injury and transection injury. Stereological analysis to measure immunohistochemical staining was performed on the scar and injury zones to detect astrocytes and the chondroitin sulphate proteoglycan NG2. **Results**: The volume fraction (Vv) of reactive astrocytes and NG2 proteoglycans increased significantly between day 3 and day 10 post injury in both *ex vivo* models. This data shows how *ex vivo* SCI models are a useful research tool allowing reduction of research cost and time involved in carrying out animal studies, as well as reducing the numbers of animals used. **Comparison with Existing Method**: This is the first evidence of an *ex vivo* stab injury model of SCI and also the first comparison of immunohistochemical staining for injury markers within stab injured and transection injured *ex vivo* slice cultures. **Conclusions**: The use of organotypic slice culture models provide a simple way to study the cellular consequences following SCI and they can also be used as a platform for potential therapeutics regimes for the treatment of SCI.

KEYWORDS: *Ex vivo* slice culture, spinal cord injury, stab injury, transection injury, reactive astrocytes, NG2 proteoglycans

1 INTRODUCTION

Based on the mechanisms of human spinal cord injury (SCI), animal models have been established and validated over many years (Kwon et al., 2004). These animal models of SCI can be classified as contusion, compression, distraction, dislocation, transection and photochemical-induced injury models (Cheriyan et al., 2014). However, the use of animals to model SCI requires extensive post-operative care, time and involves the use of animals, all of which makes an alternative model extremely attractive. The *ex vivo* slice culture system is a useful tool to maintain a 3-dimensional structure containing neurons and glial cells that represents the *in vivo* environment rather than a 2-dimensional *in vitro* system. *Ex vivo* cultures have been reported to maintain cytoarchitecture of the tissue for up to 6 weeks in culture (Pandamooz et al., 2016). The *ex vivo* slice culture system has been used to investigate of the glial-neuron interaction in 3-dimensional nigrostriatal systems investigating dopamine loss (McCaughey-Chapman and Connor, 2017) and also in iron deposition following neurodegenerative diseases (Healy et al., 2016). *Ex vivo* organotypic slice cultures have also been used to investigate the effect of new drugs in patient-specific tumor tissue (Merz et al., 2017; Parker et al., 2017).

Several organotypic spinal cord slice culture models have been developed in order to mimic the *in vivo* SCI environment and to understand the biological response following injury (Morrison et al., 1998). These *ex vivo* models include weight drop blunt injury (Krassioukov et al., 2002), transection type injuries (Pinkernelle et al., 2013; Pohland et al., 2015; Weightman et al., 2014) and chemical-induced injuries (Gerardo-Nava et al., 2014; Gerardo-Nava et al., 2013). A SCI caused by a stab injury is a rare type of injury, resulting in partial or, in some cases, complete transection of the spinal cord (O'Neill et al., 2004). A reproducible way to model a spinal cord stab injury is to cut the corticospinal tract (CST) at the dorsal column of the spinal cord using a

sharp object (Suzuki et al., 2010). The stab injury of the dorsal CST results in loss of locomotion of hind limbs and depending on the level of the injury, forelimbs can also be affected (McCaughey et al., 2016; O'Neill et al., 2004). Transection injury of the spinal cord is rarely encountered in clinical practice, however it is a very reproducible model of SCI used to investigate regeneration, degeneration, neuroplasticity and tissue engineering applications. Full transection injury models involve complete disconnection between caudal and rostral segments of the cord (Cheriyan et al., 2014).

Reactive astrocytes are one of the cellular components of the glial scar (Buffo et al., 2008; Silver and Miller, 2004; Yuan and He, 2013). Reactive astrocytes show increased expression of intermediate filaments such as Glial Fibrillary Acidic Protein (GFAP), vimentin and nestin (Adams and Gallo, 2018; Silver and Miller, 2004). This reactive astrogliosis contributes to the inhibition of axonal regeneration and the glial scar also activates NG2-positive cells, consisting of oligodendrocyte precursor cells (OPC), pericytes, non-myelinating Schwann cells, meningeal cells, microglia and macrophages surrounding the lesion site (Adams and Gallo, 2018; Hesp et al., 2017).

The aim of this study was to develop a reproducible *ex vivo* model of SCI that could be used to study components of the glial scar (in particular reactive astrocytes and NG2, one of the Chondroitin Sulphate Proteoglycans (CSPGs) upregulated after SCI). In this study, we examined two *ex vivo* organotypic slice culture models of SCI: stab injury and transection injury. We tried to mimic injury models *in vivo* by refining *ex vivo* organotypic spinal culture and evaluated these in terms of the formation of glial scar following SCI.

2 MATERIALS AND METHODS

2.1 Animals

Sprague-Dawley rats (Charles River UK Ltd, Margate, UK) were used in this study. All housing and surgical procedures carried out in this study were approval by the Animal Care Research Ethics Committee at the National University of Ireland, Galway and conformed to European Union Directive 2010/63. Postnatal day (P) 4 rat pups were sacrificed by anaesthesia with 5% Isoflurane followed by decapitation using a guillotine (Stoelting Co, Germany). The bodies were kept in sterile dishes on ice prior to spinal cord harvesting. Spinal cord isolation was performed in a class II biological safety cabinet under aseptic conditions. The skin was incised using a sterile blade #10 (Swann-Morton, England) along the midline of the dorsum. A small transverse incision was made on the sacral vertebrae. The spinal cords were flushed from the vertebral column using a 1ml syringe fitted with an 18G needle and filled with 1X ice-cold Phosphate Buffered Saline (PBS; pH 7.4) (Kennedy et al., 2013). The spinal cords were suspended in ice-cold artificial cerebrospinal fluid (aCSF; pH 7.4) composed of 126mM NaCl, 2.5mM KCl, 1.25mM $NaH_2PO_4.H_2O$, 2mM $CaCl_2.2H_2O$, 2mM $MgSO_4.7H_2O$ and 10mM glucose. The meninges were gently dissected away using sterile fine forceps in ice-cold sucrose aCSF under a stereomicroscope (Wild MZ32, Switzerland). The intact spinal cords were cut into smaller chunks approximately 1 cm in length and transferred to sterile tissue chopper discs for spinal cord slicing. Spinal cords were chopped on a tissue chopper and two different spinal cord injury models were carried out on the spinal cords: stab injury and transection injury. All slice culture was performed in a class II biological safety cabinet under aseptic conditions.

2.2 Spinal cord stab injury model

Transverse sections of spinal cord were chopped at 350µm thickness on the McIIwain tissue chopper (Mickle Laboratory Engineering Co. Ltd., USA) and tissue slices were pooled together in a petri dish in aCSF. The tissue slices were then transferred to 30mm diameter cell culture inserts (Merck Millipore, Germany) and cultured in 6 well trays (5 slices per insert). Slices were maintained in spinal cord slice culture medium consisting of: 48% MEM, 25 mM Hepes, 25% heat-inactivated horse serum, 2 mM glutamine, 1% Penicillin Streptomycin, 1% N-Acetyl L-Cysteine and 25% Hanks Balanced Salt Solution (Sigma Aldrich, Ireland) at 37^{o}C in a 5% humidified CO_2 atmosphere. All media was changed every two days. After 4 days in culture, the tissue slices were separated into a control (uninjured; 90 spinal cord tissue transverse slices) and an injury group (90 spinal cord tissue transverse slices). A stab injury was created in the slices within the injury group using a sterile 27G needle targeting the corticospinal tract of the slices located within the dorsal white matter. The anatomical region of the rat CST/dorsal white matter region was defined based on the proportion of white matter and gray matter in the transverse slices observed using the stereomicroscope. Slices were fixed at 3 days and 10 days post injury with 4% paraformaldehyde (PFA).

2.3 Spinal cord transection injury model

Longitudinal sections of spinal cord were chopped at 350µm thickness on the tissue chopper. All tissue slices were pooled together in a Petri dish. The spinal cord tissue slices were then transferred to 30 mm diameter cell culture inserts (Merck Millipore, Germany). Two slices per insert were cultured in 6 well trays containing 1ml spinal cord slice culture medium (see above). All media

was changed every two days. After 4 days in culture, the tissue slices were separated into a control group (uninjured, 36 slices) and injured group (36 slices). A transection injury was performed on the spinal cord slices within injured groups midway along the length of the tissue slices using two sterile scalpel blades #10 (Swann-Morton, England) attached to a scalpel handle. These blades were 460 µm distance apart. Spinal cord slices were fixed with 4% PFA at day 3 and day 10 post injury.

2.4 Tissue fixation and Immunohistochemistry

Spinal cord slices were fixed with 4% PFA in 1X PBS. On the day of tissue fixation the media was removed from each well and replaced with 1X PBS. The spinal cord slices were fixed with 4% PFA for 24 hours at 4^0C in 6 well trays. These slices were immunohistochemically stained for markers of reactive astrocytes (GFAP) and the CSPG NG2. The spinal cord tissue slices were washed in 1X PBS three times (5 mins per wash). The spinal cord tissue on the inserts was transferred to 24 well trays by cutting the insert membrane into pieces small enough to fit inside the 24 well tray wells. Immunohistochemical staining was performed on the tissue slices in the 24 well trays. For each antibody staining used in this study, 6 slices were used per control group and 9 slices per injured group per time point for each litter which relates to 12 pups per litter (n = 3 litters). To block nonspecific staining, the spinal cord slices were incubated with blocking buffer (10% normal goat serum (NGS) in 1X PBS with 0.5% Tween-20) for 2 hrs at room temperature. The blocking solution was replaced with primary antibody solution diluted in 1X PBS blocking buffer overnight at 4^0C. Primary antibodies used in this study were: polyclonal rabbit anti-GFAP (Dako, Denmark; 1:100) and monoclonal mouse anti-NG2 (Merck Millipore, Germany; 1:200).

After 24 hours primary antibody incubation, the slices were washed with 1X PBS three times (5 mins per wash). The slices were then incubated with secondary antibodies for 2 hours at room temperature. The secondary antibodies used in this study were: goat anti-rabbit Alexa Flour 594 (Invitrogen, UK; 1:200) and goat anti-mouse Alexa Flour 488 (Invitrogen, UK; 1:200). The slices were washed with 1X PBS three times (5 mins per wash). To counter stain the cell nuclei, the slices were incubated with 1 μg/ml 4' 6,-diamidino-2-phenylindole (DAPI; ThermoFisher Scientific) for 15 mins at room temperature. The slices were washed with 1X PBS three times (5 mins per wash) and were left in 1X PBS at 4^0C until ready for imaging. A negative control was carried out where the primary antibody was replaced with diluent buffer for the duration of the primary antibody incubation and secondary antibody was added as per other staining (see Supplementary figure 2).

2.5 Imaging

Tissue slices on Millipore inserts were inverted and placed into 35 mm glass bottom dishes (WillCo Well BV, Netherlands). The slices were mounted in 1X PBS and imaged using an Andor spinning disc confocal microscope (Andor Technology Ltd, UK). Confocal z-stack images were captured 1μm apart from the top to the bottom of the spinal cord slices using a 10X objective lens (numerical aperture 0.3) and a 20X objective lens (numerical aperture 0.5). All imaging was carried out using the same exposure time and emission gain for all the spinal cord slices.

2.6 Stereological analysis

Confocal images of each antigenic marker were examined using stereology to determine the proportion of tissue/Vv composed of immuno-positive cells using a simple point counting method (Howard and Reed, 2004). A square point grid was placed randomly on the top of the images using computer-generated grids and this grid was used to count the number of points hitting immuno-positive cells. The Vv of immuno-positive cells was calculated by dividing the number of grid intersections hitting immunoreactive cells by the total number of points hitting tissue. One projected confocal image was examined per tissue slice. For uninjured tissue slices, stereological analysis was performed on images captured away from the edge of the tissue slices. The spinal cord slices from the injured group were examined into two zones of interest: injury zone (IZ) and scar zone (SZ). IZ was defined as the centre of the lesion site and SZ was defined as a distance of 100 µm from the edge of the lesion site.

2.7 Statistics

All data collected from stereological analysis was saved in Microsoft Excel 2013 (Microsoft Office, USA). Statistical analysis was carried out using Minitab software (Minitab Incorporation, USA). All the graphs were illustrated using Graphpad Prism software (Prism 7, USA). To test for differences between the parameters examined a two-way Analysis of Variance (ANOVA) was performed followed by post hoc Tukey's test. All the statistical significance was set at probability (p) value less than 0.05, 0.01 and 0.001. All the results were presented as mean ± standard error of the mean (SEM).

3 RESULTS

The presence of GFAP, NG2 and DAPI-stained nuclei was examined in stab injured (single confocal optical images) and transection injured slice cultures (projected confocal images) at day 3 and day 10 post injury at two locations: the IZ and SZ.

3.1 Middle optical slices of confocal image stack show highest levels of cellular staining following stab injury in *ex vivo* spinal cord slices

The IZ was examined in single optical confocal images captured from the stab injured slice cultures at day 3 (Figure 1A) and day 10 (Figure 1B) post injury. The Vv of GFAP, Vv of NG2-positive cells and Vv DAPI stained nuclei in the Injury Zone (IZ) was shown to be highest in the middle confocal optical slice taken from the stack of confocal images, confirming good penetration of the antibodies into tissue slices (Figure 1C). Between day 3 and day 10 at the midway level there was a significant increase in Vv GFAP-positive cells, NG2-positive cells and DAPI-stained nuclei ($p \leq 0.001$). The DAPI-stained cells were likely composed of GFAP/NG2-positive cells as these cells increase by day 10 post injury (Figure 1C).

The SZ was also examined at day 3 and day 10 post injury (Figure 2A and 2B respectively) to determine if there were any differences in the Vv of astrocytes and NG2-positive cells. At day 3 in the middle slices there were significantly less NG2-positive cells ($p \leq 0.001$) in comparison to the Vv GFAP-positive cells and DAPI stained nuclei (Figure 2C). However, at day 10 in the midway level of confocal optical slices, there were no significant differences between Vv GFAP-positive cells, NG2-positive cells and DAPI stained nuclei. Between day 3 and day 10 at the midway level there was a significant increase in Vv GFAP-positive cells, NG2-positive cells and DAPI-stained nuclei ($p \leq 0.001$), indicating cell proliferation and/or migration between day 3 and day 10.

3.2 Increase in cell staining over time in transection injured *ex vivo* spinal cord slices

Projected stacks of confocal images showing transection injured slices of spinal cord were examined at day 3 (Figure 3A) and day 10 (Figure 3B) post injury for markers of GFAP, NG2 and DAPI stained nuclei in the IZ of tissue slices. The distance between the two cut edges of spinal cord was observed to decrease over time (Supplementary figure 1). In the IZ on day 3 and day 10, there were no significant differences between Vv GFAP and Vv NG2 positive cells, although there were considerably more DAPI stained cells present compared to these GFAP and NG2-positive cells (Figure 3C). Between day 3 and 10, there was a significant increase in Vv GFAP-positive cells and NG2-positive cells.

The SZ of transection injured spinal cord slices was examined at day 3 and day 10 (Figure 4A and 4B respectively). On day 3, there was significantly higher Vv of GFAP-positive cells compared with NG2-positive cells (Figure 4C). An increase in all cellular staining was observed between day 3 and day 10 post injury (Figure 4C).

4 DISCUSSION

The use of *ex vivo* models of SCI allows researchers to mimic injury models *in vivo*. *Ex vivo* models support the 3R's concept of replacement, reduction and refinement of animal use in SCI research. The examination of cellular changes in the spinal cord slice cultures allows real time study of the interaction of heterogeneous populations of cell types. The cell populations are maintained within *ex vivo* slice cultures with 3-dimensional connections between neurons and supporting cells (Doussau et al., 2017). The cellular architecture is preserved and one can

investigate treatment strategies in 3-dimensional microenvironments. However, there are limitations in the slice culture model as there is no circulating blood and therefore a limited ability to examine immune responses. The accumulation of microglia/macrophages occurs at the edges of slices due to damage caused by the dissection and tissue chopping procedures (Fernandez-Zafra *et al*., 2017). We optimised our culture protocol by delaying any treatment until day 4 to avoid immune cell involvement from the tissue harvest procedure. In this study, two *ex vivo* slice culture models of SCI were examined (stab injury and transection injury) and the expression of GFAP-positive astrocytes and NG2-positive cells was observed in the SZ and IZ. Postnatal animals were chosen in these experiments as they have better morphology, increased survival and more stable susceptibility in lesion models compared to adult slices (Humpel, 2015). Although transection injuries have been examined in *ex vivo* spinal cord slices (Pinkernelle et al., 2013; Pohland et al., 2015; Weightman et al., 2014), to the best of our knowledge this is the first report on *ex vivo* spinal cord stab injury.

In the stab injury the Vv of each cell marker was measured in confocal optical slices at top, midway through and bottom of the confocal image stacks. As expected, the GFAP and NG2 were expressed at all levels of confocal optical slices (top, midway and bottom). The majority of staining was observed at the midway level in the stab injury model (Figure 1C), therefore it was decided to use projected series of confocal images for further analysis when we progressed on to the transection model. The Vv of GFAP-positive cells and NG2-positive cells appeared to account for the majority of DAPI stained nuclei present in the IZ (Figure 1C). This suggests that the cells residing in the IZ and cells migrating to the IZ may be astrocytes, reactive astrocytes, NG2-expressing cells as well as other cell types responding to the injury. The increase in GFAP expression observed here between 3 and 10 days was also observed in previous studies of slice

cultures (Pohland et al., 2015) and *in vivo* studies (Donnelly et al., 2012; Moon et al., 2000). Increased expression of NG2 was also observed over time here, which concurs with the study of Jones *et al*. who reported that NG2 is upregulated between 24 hours and 3 days after injury in animal studies, peaking at 7 days post injury (Jones et al., 2002).

The Vv of cellular staining observed in the transection injury model showed a similar pattern of GFAP and NG2 expression in the SZ of transected spinal cord slices at day 3 and 10 (Figure 4C). The Vv of GFAP and NG2 increased as reported previously in slice cultures (Pohland et al., 2015) and in an *in vivo* model of transection injury (Moon et al., 2000). Resident SZ cell proliferation and migration from adjacent regions into the SZ may account for the increase in GFAP-positive cells, NG2-positive cells and DAPI stained nuclei in the transection lesion gap by day 10 (Figure 3C).

In summary, both of the models of SCI presented here have fulfilled the 3R's concept of replacement, reduction and refinement of animal use in SCI research models. Each model generated a consistent, easily reproducible and graded injury that represents SCI pathology. The use of stab injury *ex vivo* is the reproducible way to model a spinal cord injury with cut at the particular dorsal corticospinal tract. The transection *ex vivo* model showed the ability to study the transection gap and expression of different cell types that may help to incorporate strategies to promote axonal outgrowth following SCI *ex vivo*. These *ex vivo* models are useful as a platform for studying glial scarring and potential SCI treatment.

ACKNOWLEDGEMENTS

The authors acknowledge the facilities, scientific and technical assistance (Mr Mark Canney and Dr Kerry Thompson) of the Centre for Microscopy and Imaging at the National University of Ireland, Galway (www.imaging.nuigalway.ie), a facility which is co-funded by the Irish Government's Programme for Research in Third Level Institutions, Cycles 4 and 5, National Development Plan 2007-2013. Funding for this project was provided by the Malaysia Ministry of Education and the College of Medicine, Nursing and Health Science at NUI Galway.

REFERENCES

Adams KL, Gallo V. The diversity and disparity of the glial scar. Nature Neuroscience, 2018; 21: 9-15.

Buffo A, Rite I, Tripathi P, Lepier A, Colak D, Horn AP, Mori T, Gotz M. Origin and progeny of reactive gliosis: A source of multipotent cells in the injured brain. Proc Natl Acad Sci U S A, 2008; 105: 3581-6.

Cheriyan T, Ryan DJ, Weinreb JH, Cheriyan J, Paul JC, Lafage V, Kirsch T, Errico TJ. Spinal cord injury models: a review. Spinal Cord, 2014; 52: 588-95.

Ciavatta VT, Bichler EK, Speigel IA, Elder CC, Teng SL, Tyor WR, Garcia PS. In vitro and Ex vivo Neurotoxic Effects of Efavirenz are Greater than Those of Other Common Antiretrovirals. Neurochem Res, 2017.

Donnelly EM, Madigan NN, Rooney GE, Knight A, Chen B, Ball B, Kinnavane L, Garcia Y, Dockery P, Fraher J, Strappe PM, Windebank AJ, O'Brien T, McMahon SS. Lentiviral vector delivery of short hairpin RNA to NG2 and neurotrophin-3 promotes locomotor recovery in injured rat spinal cord. Cytotherapy, 2012; 14: 1235-44.

Doussau F, Dupont JL, Neel D, Schneider A, Poulain B, Bossu JL. Organotypic cultures of cerebellar slices as a model to investigate demyelinating disorders. Expert Opin Drug Discov, 2017; 12: 1011-22.

Fernandez-Zafra T, Codeluppi S, Uhlén P. An *ex vivo* spinal cord injury model to study ependymal cells in adult mouse tissue. Exp Cell Res. 2017; 357(2): 236-242.

Gerardo-Nava J, Hodde D, Katona I, Bozkurt A, Grehl T, Steinbusch HW, Weis J, Brook GA. Spinal cord organotypic slice cultures for the study of regenerating motor axon interactions with 3D scaffolds. Biomaterials, 2014; 35: 4288-96.

Gerardo-Nava J, Mayorenko, II, Grehl T, Steinbusch HW, Weis J, Brook GA. Differential pattern of neuroprotection in lumbar, cervical and thoracic spinal cord segments in an organotypic rat model of glutamate-induced excitotoxicity. J Chem Neuroanat, 2013; 53: 11-7.

Greenwood K, Butt AM. Evidence that perinatal and adult NG2-glia are not conventional oligodendrocyte progenitors and do not depend on axons for their survival. Mol Cell Neurosci, 2003; 23: 544-58.

Healy S, McMahon J, Owens P, FitzGerald U. Significant glial alterations in response to iron loading in a novel organotypic hippocampal slice culture model. Sci Rep, 2016; 6: 36410.

Hesp ZC, Yoseph RY, Suzuki R, Wilson C, Nishiyama A, McTigue DM. Proliferating NG2 cell-dependent angiogenesis and scar formation alter axon growth and functional recovery after spinal cord injury in mice. The Journal of neuroscience : the official journal of the Society for Neuroscience, 2017.

Howard V, Reed M. Unbiased Stereology: Three-Dimensional Measurement in Microscopy. Taylor & Francis, 2004.
Humpel C. Organotypic brain slice cultures: A review. Neuroscience, 2015; 305: 86-98.

Jones LL, Yamaguchi Y, Stallcup WB, Tuszynski MH. NG2 is a major chondroitin sulfate proteoglycan produced after spinal cord injury and is expressed by macrophages and oligodendrocyte progenitors. J Neurosci, 2002; 22: 2792-803.

Kennedy HS, Jones C, 3rd, Caplazi P. Comparison of standard laminectomy with an optimized ejection method for the removal of spinal cords from rats and mice. J Histotechnol, 2013; 36: 86-91.
Krassioukov AV, Ackery A, Schwartz G, Adamchik Y, Liu Y, Fehlings MG. An in vitro model of neurotrauma in organotypic spinal cord cultures from adult mice. Brain Res Brain Res Protoc, 2002; 10: 60-8.

McCaughey EJ, Purcell M, Barnett SC, Allan DB. Spinal Cord Injury Caused by Stab Wounds: Incidence, Natural History, and Relevance for Future Research. J Neurotrauma, 2016; 33: 1416-21.

McCaughey-Chapman A, Connor B. Rat brain sagittal organotypic slice cultures as an ex vivo dopamine cell loss system. Journal of neuroscience methods, 2017; 277: 83-7.

Merz L, Hobel S, Kallendrusch S, Ewe A, Bechmann I, Franke H, Merz F, Aigner A. Tumor tissue slice cultures as a platform for analyzing tissue-penetration and biological activities of nanoparticles. Eur J Pharm Biopharm, 2017; 112: 45-50.

Moon LDF, Brecknell JE, Franklin RJM, Dunnett SB, Fawcett JW. Robust Regeneration of CNS Axons through a Track Depleted of CNS Glia. Exp Neurol, 2000; 161: 49-66.

Morrison B, 3rd, Saatman KE, Meaney DF, McIntosh TK. In vitro central nervous system models of mechanically induced trauma: a review. J Neurotrauma, 1998; 15: 911-28.

O'Neill S, McKinstry CS, Maguire SM. Unusual stab injury of the spinal cord. Spinal Cord, 2004; 42: 429-30.
Pandamooz S, Nabiuni M, Miyan J, Ahmadiani A, Dargahi L. Organotypic Spinal Cord Culture: a Proper Platform for the Functional Screening. Mol Neurobiol, 2016; 53: 4659-74.

Parker JJ, Lizarraga M, Waziri A, Foshay KM. A Human Glioblastoma Organotypic Slice Culture Model for Study of Tumor Cell Migration and Patient-specific Effects of Anti-Invasive Drugs. J Vis Exp, 2017.

Pinkernelle J, Fansa H, Ebmeyer U, Keilhoff G. Prolonged minocycline treatment impairs motor neuronal survival and glial function in organotypic rat spinal cord cultures. PLoS One, 2013; 8: e73422.

Pohland M, Glumm R, Stoenica L, Holtje M, Kiwit J, Ahnert-Hilger G, Strauss U, Brauer AU, Paul F, Glumm J. Studying axonal outgrowth and regeneration of the corticospinal tract in organotypic slice cultures. J Neurotrauma, 2015.

Silver J, Miller JH. Regeneration beyond the glial scar. Nat Rev Neurosci, 2004; 5: 146-56.

Suzuki M, Klein S, Wetzel EA, Meyer M, McHugh J, Tork C, Hayes A, Svendsen CN. Acute glial activation by stab injuries does not lead to overt damage or motor neuron degeneration in the G93A mutant SOD1 rat model of amyotrophic lateral sclerosis. Exp Neurol, 2010; 221: 346-52.

Weightman AP, Pickard MR, Yang Y, Chari DM. An in vitro spinal cord injury model to screen neuroregenerative materials. Biomaterials, 2014; 35: 3756-65.

Yuan YM, He C. The glial scar in spinal cord injury and repair. Neurosci Bull, 2013; 29: 421-35.

Figure captions

Figure 1: IZ of stab injured *ex vivo* spinal cord slices. Photomicrographs show single optical confocal images of GFAP (i), NG2 (ii) and DAPI (iii) at the top level of a confocal image stack at day 3 (A) and day 10 (B) post stab injury. White asterisk, * =IZ; Dashed lines separate the region of interest examined: IZ. Scale bar = 100 µm. (C) Graph shows the proportion of GFAP, NG2 and DAPI in the IZ of injured slices within the IZ at top, midway-point and bottom of confocal image stacks. Mean ± SEM. *$p \leq 0.001$ significant increase from day 3 group. ∞ = significantly different to top and bottom confocal images. † = significantly different to DAPI at that level. The mean differences were analysed using Two-way ANOVA. n=1 litter (12 pups) which relates to 45 slices per control group per time-point and 45 slices per injured group per time-point.

Figure 2: SZ of stab injured *ex vivo* spinal cord slices. Photomicrographs show single optical confocal images of GFAP (i), NG2 (ii) and DAPI (iii) at the top level of a confocal image stack at day 3 (A) and day 10 (B) post stab injury. White asterisk, * =SZ; Dashed lines separate the region of interest examined: IZ. Scale bar = 100 µm. (C) Graph shows the proportion of GFAP, NG2 and DAPI in the SZ of injured slices at top, midway-point and bottom of confocal image stacks. Mean ± SEM. *=$p \leq 0.01$ significant increase from day 3. ∞ = significantly different to top and bottom confocal images. † = significantly different to DAPI at day 3 time point at that level. The mean differences were analysed using Two-way ANOVA. n=1 litter (12 pups) which relates to 45 slices per control group per time-point and 45 slices per injured group per time-point.

Figure 3: IZ of transection injured *ex vivo* spinal cord slices. Photomicrographs show single optical confocal images of of GFAP (i), NG2 (ii), and DAPI (iii) at day 3 (A) and day 10 (B) post injury. White asterisk, * =IZ; Scale bar = 200 µm. (C) Graph show the proportion of tissue composed of GFAP, NG2 and DAPI stained cells in the IZ of transection injured slices. Mean ± SEM. p≤ 0.01, *=p≤ 0.001 significant increase from day 3. † = significantly different to DAPI. The mean differences were analysed using Two-way ANOVA. n=1 litter (12 pups) which relates to 45 slices per control group per time-point and 45 slices per injured group per time-point.

Figure 4: SZ of transection injured *ex vivo* spinal cord slices. Photomicrographs show single optical confocal images of GFAP (i), NG2 (ii), and DAPI (iii) at day 3 (A) and day 10 (B) post transection injury. White asterisk, * = SZ; Dashed lines separate the region of interest examined: SZ. Scale bar=200 µm. (C) Graph shows the proportion of tissue composed of GFAP, NG2 and DAPI in the SZ of transection injured slices. Mean ± SEM.*=p≤ 0.001 significant increase from day 3. The mean differences were analysed using Two-way ANOVA. n=1 litter (12 pups) which relates to 45 slices per control group per time-point and 45 slices per injured group per time-point.

Supplementary figure 1: Transection gap distance in *ex vivo* transection injured spinal cord slices. Photomicrographs show representative phase contrast images of transection injured spinal cord slices at day 3 (Ai) and day 10 (Aii) after transection injury. Scale bar = 500 µm. Graph shows transected gap distance at day 3 and day 10 (B). Mean ± SEM. The mean differences were analysed using Two-way ANOVA. n=1 litter (12 pups) which relates to 45 slices per control group per time-point and 45 slices per injured group per time-point.

Supplementary figure 2: Immunohistochemical staining negative control sample image. Photomicrograph show representative single optical confocal images of transection injured spinal cord slice used as a negative control in immunohistochemical staining. Blue nuclei are stained with DAPI. White asterisk, * = IZ; Dashed lines separate the region of interest examined. Scale bar=100 µm.

Graphical abstract

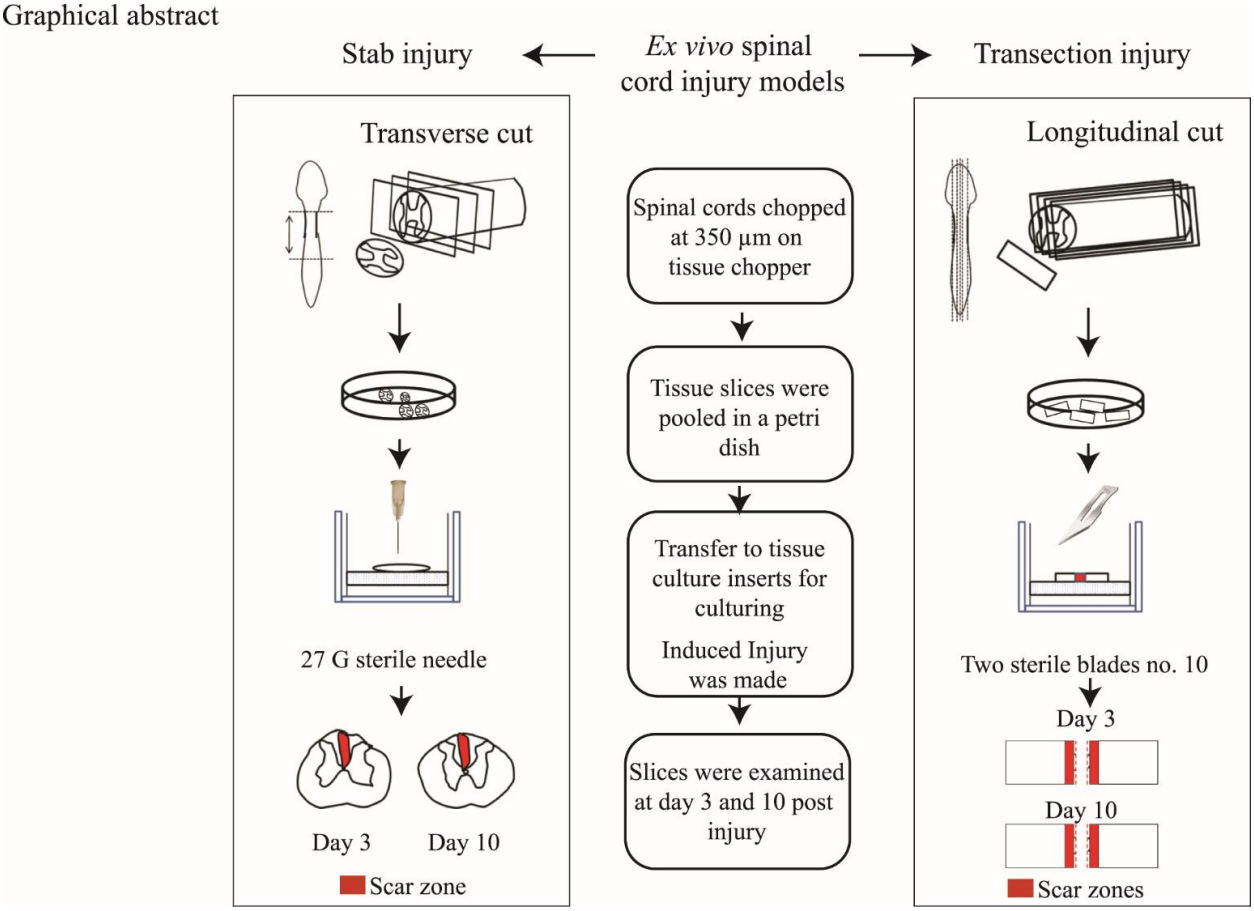

Figure 1

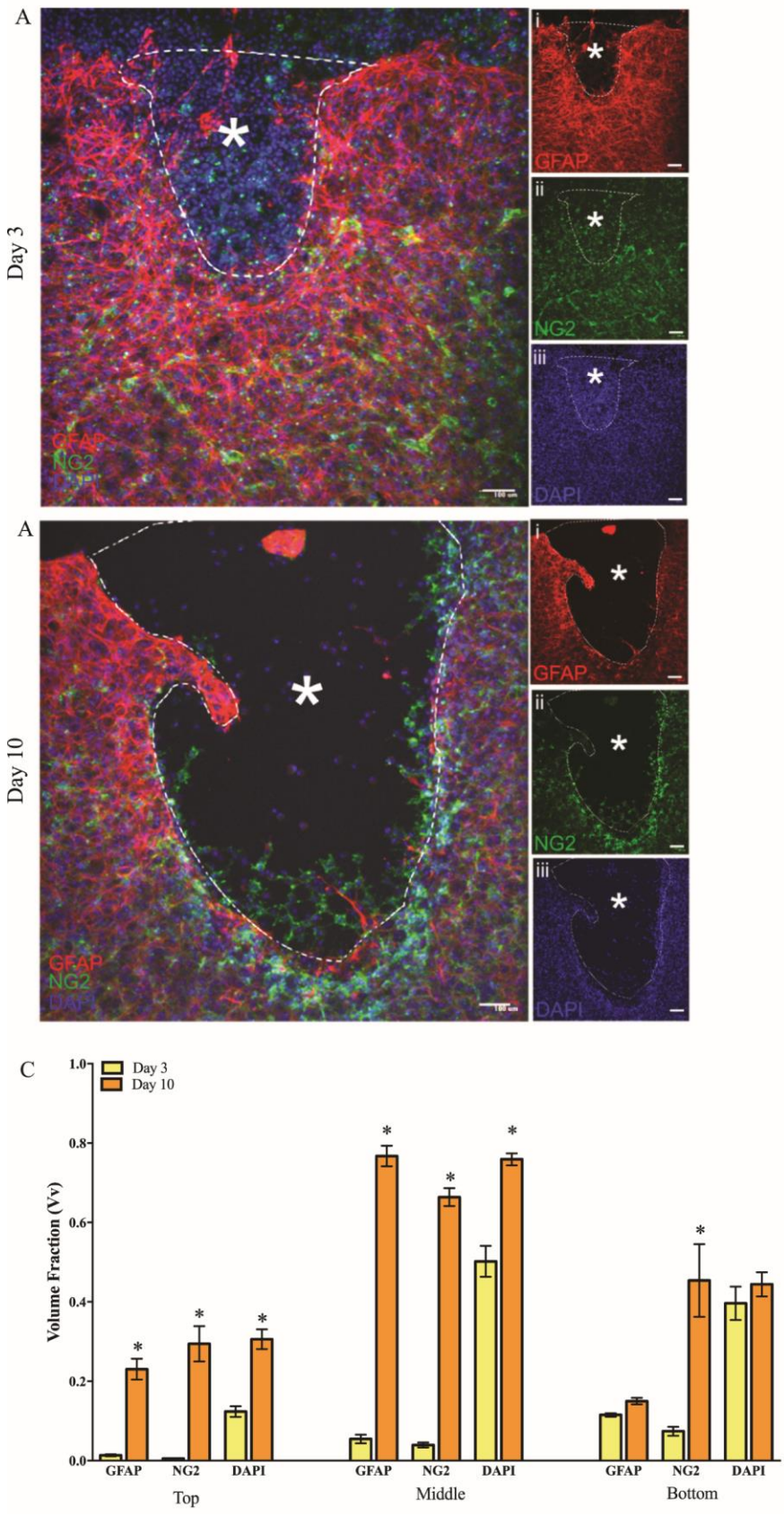
A
Day 3
i
GFAP
ii
NG2
iii
DAPI
GFAP
NG2
A
Day 10
i
GFAP
ii
NG2
iii
DAPI
GFAP
NG2
C
Day 3
Day 10
Volume Fraction (Vv)
1.0
0.8
0.6
0.4
0.2
0.0
GFAP
NG2
DAPI
Top
GFAP
NG2
DAPI
Middle
GFAP
NG2
DAPI
Bottom

Figure 2

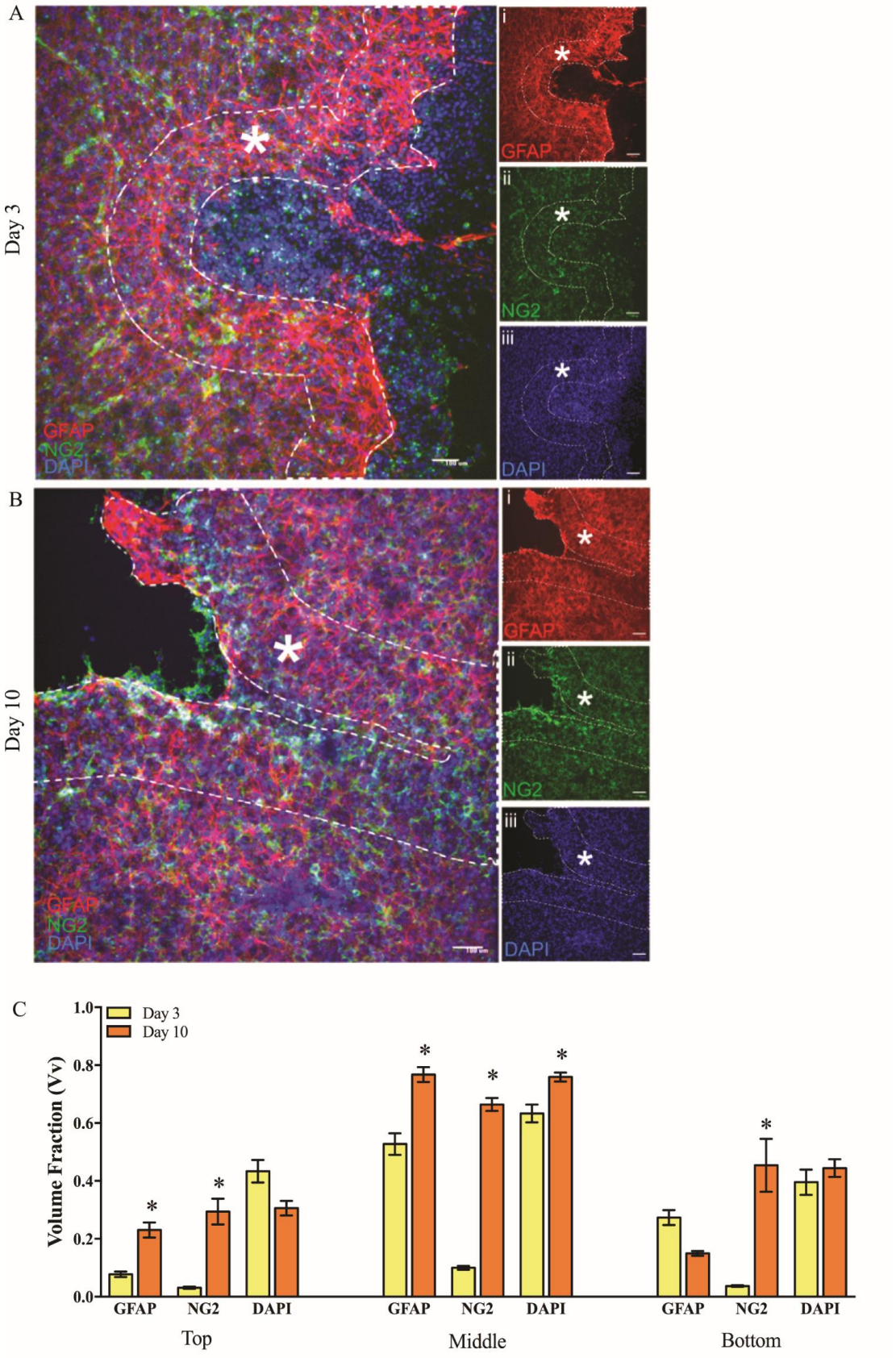
A
Day 3
GFAP
NG2
DAPI
i
GFAP
ii
NG2
iii
DAPI
B
Day 10
GFAP
NG2
DAPI
i
GFAP
ii
NG2
iii
DAPI
C
Day 3
Day 10
Volume Fraction (Vv)
1.0
0.8
0.6
0.4
0.2
0.0
GFAP
NG2
DAPI
Top
Middle
Bottom

Figure 3

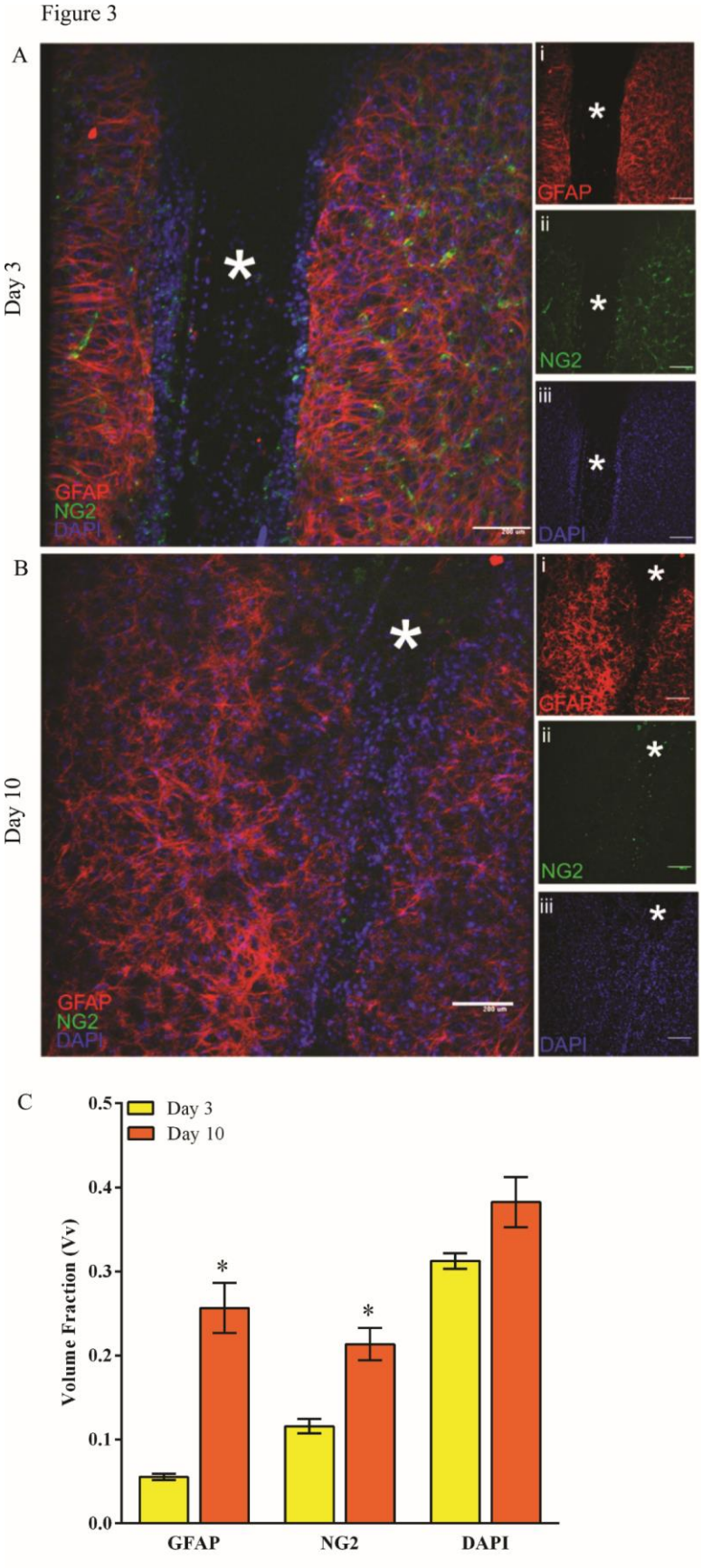
A
Day 3
GFAP
NG2
DAPI
i
GFAP
ii
NG2
iii
DAPI
B
Day 10
GFAP
NG2
DAPI
i
GFAP
ii
NG2
iii
DAPI
C
Day 3
Day 10
Volume Fraction (Vv)
0.0
0.1
0.2
0.3
0.4
0.5
GFAP
NG2
DAPI

Figure 4

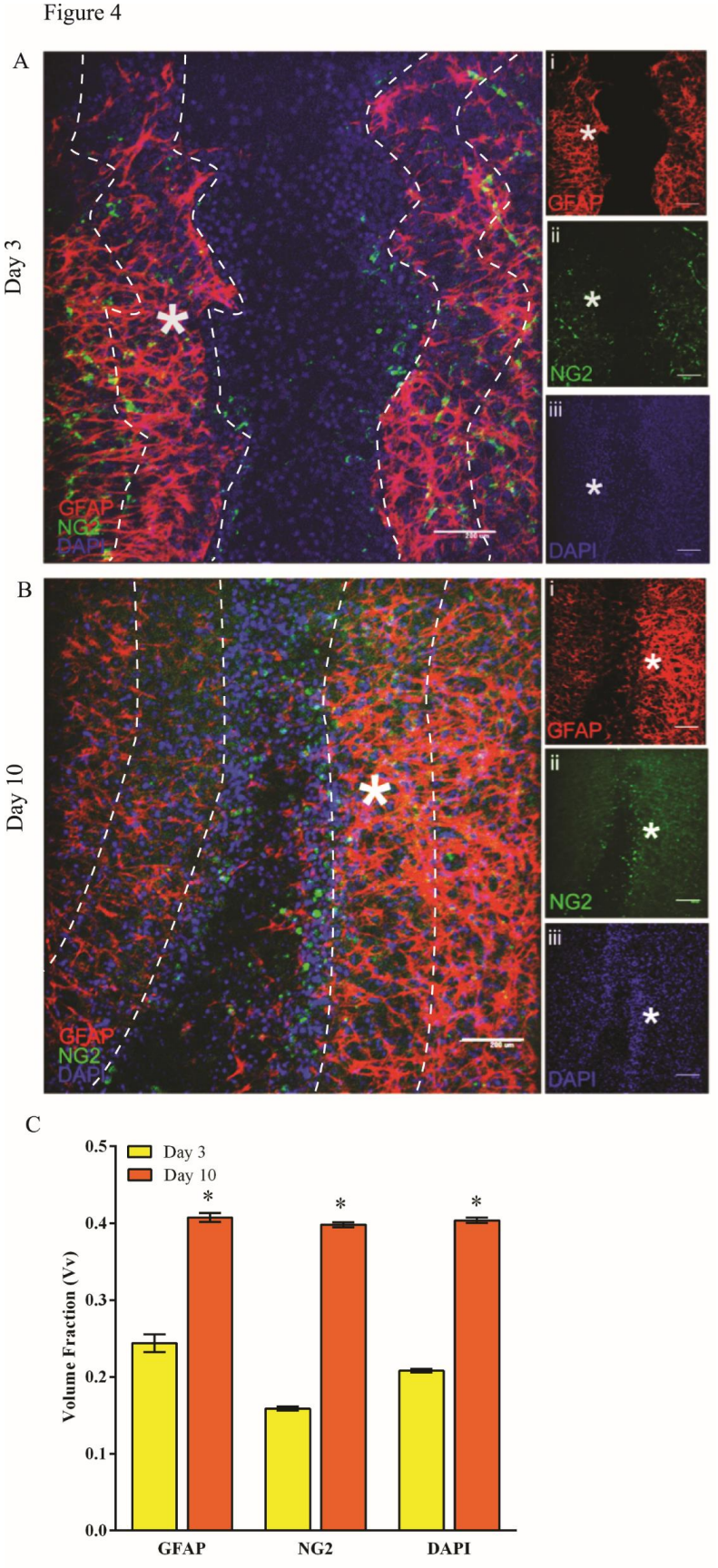
A
Day 3
i
GFAP
ii
NG2
iii
DAPI
GFAP
NG2
DAPI
B
Day 10
i
GFAP
ii
NG2
iii
DAPI
GFAP
NG2
DAPI
C
Day 3
Day 10
Volume Fraction (Vv)
0.5
0.4
0.3
0.2
0.1
0.0
GFAP
NG2
DAPI

Supplementary figure 1

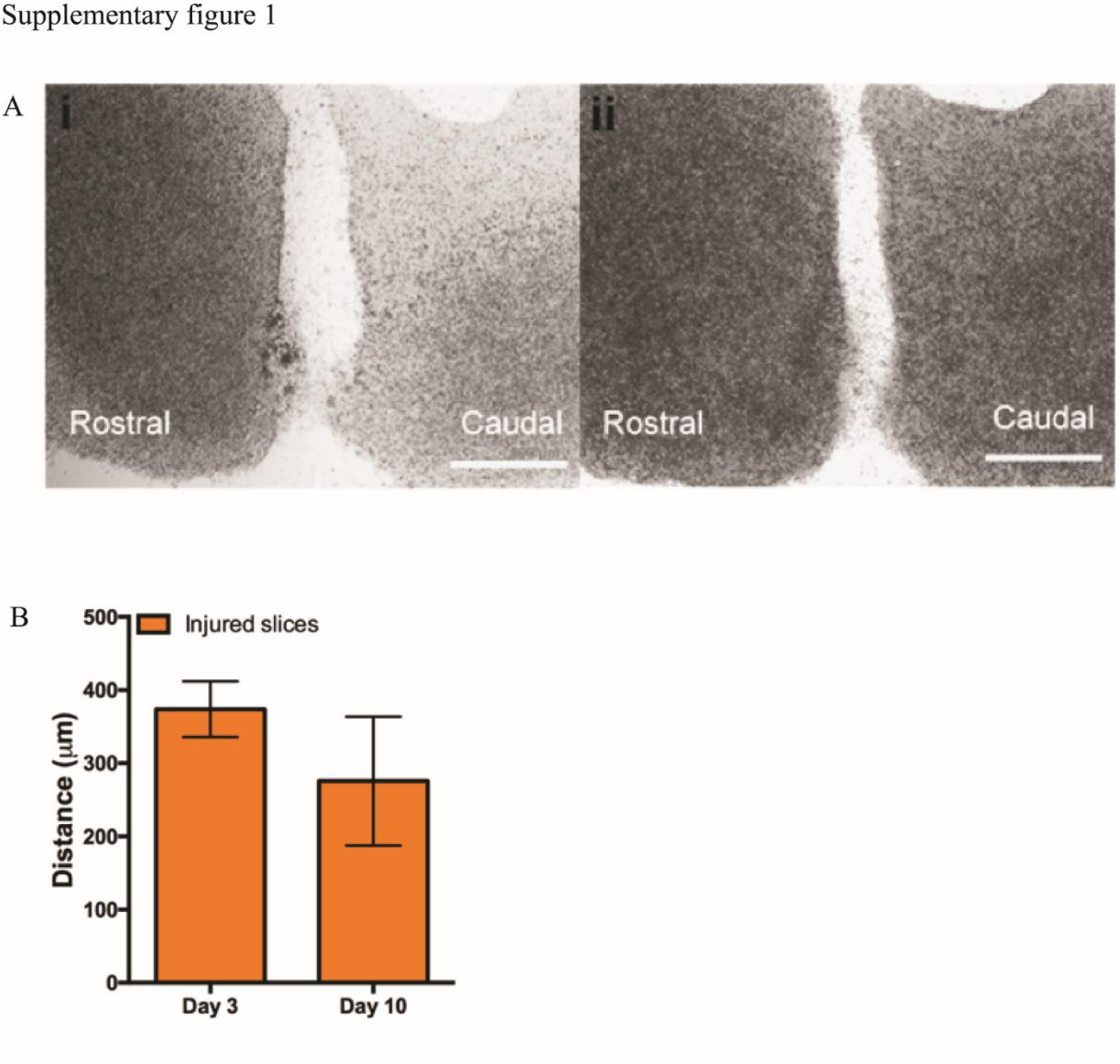

Supplementary figure 2